Columbia University in the City of New York

LAMONT GEOLOGICAL OBSERVATORY

PALISADES, NEW YORK

ANALYSIS OF DIFFUSION OF DYE PATCHES IN THE OCEAN

Report prepared by: Takashi Ichiye
Hayato Iida
Noel B. Plutchak

Technical Report No. CU-8-64 to the Atomic Energy Commission
Contract AT(30-1)2663

January, 1964

LAMONT GEOLOGICAL OBSERVATORY
(Columbia University)
Palisades, New York

ANALYSIS OF DIFFUSION OF DYE PATCHES IN THE OCEAN

Report prepared by: Takashi Ichiye
Hayato Iida
Noel B. Plutchak

Technical Report No. CU-8-64 to the Atomic Energy Commission
Contract AT(30-1)2663

January, 1964

ABSTRACT

The data of dye patch experiments made off New Jersey and on the Bahama Banks are analyzed. The second moment of the concentration distribution increases with square of time in the initial stage and with cube of time later, in agreement with a theory of a two-particle problem. In order to explain the curved trailing part of the dye patches, refraction of a submerged object is treated theoretically. It is found that the effect of refraction may cause a curved image, but the curvature due to refraction is much smaller than actually observed. The vertically differential advection as the main cause of the curved pattern is treated analytically, and the result is applied to computing vertical eddy viscosity from the observed curved trailing portion of dye patches. The mechanism of striated patterns of dye patches is discussed from the point of view of hydrodynamic instability and of rolling up of streak lines.

I. INTRODUCTION

As emphasized by Frenkiel (1958), turbulence is a normal condition of fluid motion encountered in nature; and laminar motion, to which more than 95% of Sir Horace Lamb's exhaustive Hydrodynamics was devoted, is rather exceptional. Almost any water movement in the ocean, from the general circulation to sound waves, is more or less influenced by turbulence. Therefore, it is rather surprising that very few studies have been done on oceanic turbulence, although there has been substantial progress in recent years, both in theoretical and experimental researches on turbulence in general and to some degree atmospheric turbulence in particular.

Among others, there are two main reasons for the lack of progress in studying oceanic turbulence. One is that measurement of quantities in the ocean pertinent to turbulence is complicated, owing to technical difficulties of instrumentation and the rigors of oceanographic field work. The other is a theoretical difficulty. A theory of isotropic homogeneous turbulence was well developed (Batchelor, 1953), and it was found that most of the results are valid in the atmospheric turbulence. However, in the ocean such validity is dubious, partly due to the horizontal boundaries and free surface, both of which have no counterpart in the atmosphere, and partly due to the condition that the energy of turbulence is mostly supplied through the free surface in the form of wind stresses.

However, from another point of view, these liabilities for studying oceanic turbulence become assets. In the experimental phase, measurement of turbulence characteristics by Eulerian methods is far more difficult in the ocean than in the atmosphere, since current meters capable of recording small fluctuations of currents in the sea are yet to be made. However, Lagrangian methods can be more easily utilized in the ocean than in the atmosphere. For

instance, tracing of current drogues can be done relatively easily for a long period of time and will give fairly accurate pictures of flow patterns and their fluctuations, while tracking of pilot balloons in the atmosphere is feasible only for a short time and is not accurate enough to determine fluctuations of the wind. Diffusion of dye patches has also become a powerful tool in studying horizontal turbulence in the ocean, owing to recently developed techniques for measuring concentration and for navigation. Dye patches can be followed for a fairly long time and movements of patches also occur, in most cases, almost horizontally with a small spreading along the vertical direction. These are remarkable advantages, considering the case of diffusion of smoke, since one cannot make experiments of large scale diffusion by using smoke more than a few hours without facing a charge of willful contamination of the air.

As for complications arising from the existence of horizontal boundaries and free surface, we may consider that the ocean provides an ideal natural laboratory for turbulence with different scales from several meters to thousands of kilometers (Frenkiel, 1962). Deviation from the homogeneous, isotropic turbulence in the ocean poses challenging problems to theoreticians.

The experiments described in this report were made on the shelf off New Jersey and on the Bahama Banks. In these experiments twenty to fifty gallons of solution of Rhodamine B dye was introduced. The concentration of dye in the patches was measured continuously with a standard Turner Model III fluorometer, while a research vessel made several crossings of the patch within a period of a few hours. Aerial photographs of dye patches were taken from a light plane at ten minute intervals. Technical details of dye sampling methods, navigation methods, and aerial photography have already been explained in a previous report (Costin, Davis, Gerard and Katz, 1963),

which is referred to hereafter as ENY.

This paper presents analysis and theoretical considerations on the experiments in two areas, on the Bahama Banks and off New Jersey. These two areas are representative of oceanic regions with different turbulence characteristics. The Bahama Banks are extremely shallow with uniform depth, and the level of background turbulence (horizontal components) is correspondingly low. The sea off New Jersey is typical of the Continental Shelf, and the background turbulence energy is higher than on the Bahama Bank.

II. TWO PARTICLE MODEL OF DYE PATCH DIFFUSION

The results of diffusion experiments off New Jersey (ENY) and on the Bahama Bank (Costin, 1963) indicated that the patterns of dye patches were complicated and dissimilar to those predicted by existing diffusion theories. Particularly, striated patterns and elongation of patches are notable features which are not compatible with a model of diffusion by isotropic turbulence. However, when the logarithm of concentration is plotted against the area enclosed by the contour of that concentration, there is a linear relationship in most cases of these experiments (ENY). Therefore, the procedure of using areas enclosed by contours, instead of linear distances, may provide some kind of averaging process, on which the conventional theories of turbulent diffusion are based. When equivalent radii r_e is defined as equal to $\sqrt{A/\pi}$, where A is the area enclosed by a contour, the relationship between concentration C and r_e is expressed by:

$$C = C_m \exp\left(-\pi r_e^2 / \pi \alpha^2\right) \qquad (1)$$

where C_m is the maximum concentration and α^2 is the second moment of the concentration distribution.

Diffusion from an instantaneous source which is moving with a general current is defined as relative diffusion and is discussed approximately as two particle problem (Batchelor, 1950; Gifford, 1957). However, it is necessary to discuss this type of diffusion as a many particle problem. The difficulty in the many particle problem lies in the fact that the Lagrangian correlation functions for turbulent velocities are not yet obtained. A simple reason for this difficulty can be explained as follows:

Consider that N particles are released from a point initially. It is assumed that there is no mean current. The x-coordinate of the i-th particle at time t is expressed with $x_i(t)$. The average with N particles is represented by the bar. Then at time t,

$$\frac{d}{dt}\overline{x^2(t)} = \frac{1}{N}\sum_i \frac{d}{dt}x_i^2(t) = \frac{1}{N}\sum_i 2x_i(t)u_i(t)$$
$$= \frac{1}{N}\sum_i 2\int_0^t u_i(\tau)d\tau \cdot u_i(t) \qquad (2)$$

or:
$$\frac{d}{dt}\overline{x^2(t)} = 2\int_0^t \overline{u(\tau)u(t)}\,d\tau \qquad (2')$$

where u_i is the x-component of the velocity of the i-th particle. If all the particles are constrained on the x-axis, as in the case of the ordinary one particle problem, $\overline{u(\tau)u(t)}$ is the correlation function which depends $(t-\tau)$ only in homogeneous turbulent flow. However, the velocities $u_i(t)$ and $u_i(\tau)$ are not only dependent on the time, but also on the positions of the i-th particle $\vec{x}_i(t)$ and $\vec{x}_i(\tau)$. Therefore we have to write:

$$\overline{u(t)u(\tau)} = \frac{1}{N}\sum u_i\{t, \vec{x}_i(t)\}u_i\{\tau, \vec{x}_i(\tau)\} \qquad (3)$$

Equation (3) indicates that the correlation function $u(t)u(\tau)$ is, indeed, dependent on $\vec{x_i}(t)$ and $\vec{x_i}(\tau)$.

Batchelor (1950) treated the two particle problem from a basis of dimensional analysis instead of going into details of the Lagrangian correlation (3). According to his theory, the relative motion of two particles which are released at the distance ξ_0 is governed by turbulence of the inertial subrange if the Reynolds' number of the turbulence is sufficiently large, as in the ocean. In the inertial subrange, energy of turbulence is transferred from larger eddies to smaller ones due to inertial forces, and energy of the smaller eddies is finally dissipated by viscosity at the rate ε. Therefore, physical quantities pertinent to the process in this range are ε and ξ_0, since viscosity affects only the smallest eddies. Then dimensional reasoning leads to the relation:

$$\frac{d}{dt}\overline{\xi^2(t)} = \varepsilon t^2 F\left(\xi_0/\varepsilon^{\frac{1}{2}} t^{\frac{3}{2}}\right) \tag{4}$$

for the rate of change of mean square separation $\xi^2(t)$, where F is a universal function. When t is sufficiently small, the relative velocity of the two particles remains constant, and thus the left-hand side of (4) is proportional to t (Batchelor, 1956), so that:

$$\frac{d}{dt}\overline{\xi^2(t)} = \text{Const} \cdot t\,(\varepsilon \xi_0)^{\frac{2}{3}} \tag{5}$$

or:

$$\overline{\xi^2(t)} = \text{Const} \cdot t^2 (\varepsilon \xi_0)^{\frac{2}{3}} + \xi_0^2 \tag{6}$$

On the other hand, if t is so large that the relative motion of the two particles no longer depends on the initial separation ξ_0, equation (4) becomes:

$$\frac{d}{dt}\overline{\xi^2(t)} = \text{const.}\ \varepsilon t^2 \tag{7}$$

or: $$\overline{\xi^2(t)} = \text{const.}\ \varepsilon\, t^3 \tag{8}$$

Since the constant α^2 in equation (1) is proportional to $\overline{\xi^2(t)}$ (Gifford, 1957), validity of relations (6) and (8) can be tested by plotting α^2, determined from the curves of concentration versus area, against time. The result is shown in Figure 1, in which the values of α^2 determined from the experiments off New Jersey and on the Bahama Bank are plotted in logarithmic scale. Equation (6) can be written as:

$$\overline{\xi^2(t)} = \text{const.}\ (t^2 + t_o^2) \tag{6'}$$

where t_o is the constant which is proportional to $\varepsilon^{-\frac{2}{3}}\, \xi_o^{\frac{1}{3}}$. Since there is no deductive method to determine constants in equations (6) and (8), we have to be satisfied with comparing the trend of theoretical curves with the values determined from the data. Figure 1 indicates that the rate of increase of α^2 with time agrees with the theoretical formula (8) for a large time interval. In order to compare equation (6') with the data, curves are plotted for t_o = 0, 200 min., 300 min. and 500 min., respectively. Since t_o depends on the initial condition of dye patches, different sets of experimental data correspond to different values of t_o in the first stage, which is represented by equation (6) or (6'). It can be seen clearly that there is a second stage corresponding to (8), except in the data of the South Bahama Bank. This figure also indicates that the turbulent energy dissipation ε is larger in the area off New Jersey than on the Bahama Bank, since the values of α^2 are larger in the former area for the same range of t. This is plausible, because the shallow water of the Bahama Bank inhibits full development of turbulence.

or: $$\overline{\xi^2(t)} = \text{const.}\ \varepsilon\, t^3 \tag{8}$$

Since the constant α^2 in equation (1) is proportional to $\overline{\xi^2(t)}$ (Gifford, 1957), validity of relations (6) and (8) can be tested by plotting α^2, determined from the curves of concentration versus area, against time. The result is shown in Figure 1, in which the values of α^2 determined from the experiments off New Jersey and on the Bahama Bank are plotted in logarithmic scale. Equation (6) can be written as:

$$\overline{\xi^2(t)} = \text{const.}\ (t^2 + t_o^2) \tag{6'}$$

where t_o is the constant which is proportional to $\varepsilon^{-\frac{2}{3}}\, \xi_o^{\frac{1}{3}}$. Since there is no deductive method to determine constants in equations (6) and (8), we have to be satisfied with comparing the trend of theoretical curves with the values determined from the data. Figure 1 indicates that the rate of increase of α^2 with time agrees with the theoretical formula (8) for a large time interval. In order to compare equation (6') with the data, curves are plotted for t_o = 0, 200 min., 300 min. and 500 min., respectively. Since t_o depends on the initial condition of dye patches, different sets of experimental data correspond to different values of t_o in the first stage, which is represented by equation (6) or (6'). It can be seen clearly that there is a second stage corresponding to (8), except in the data of the South Bahama Bank. This figure also indicates that the turbulent energy dissipation ε is larger in the area off New Jersey than on the Bahama Bank, since the values of α^2 are larger in the former area for the same range of t. This is plausible, because the shallow water of the Bahama Bank inhibits full development of turbulence.

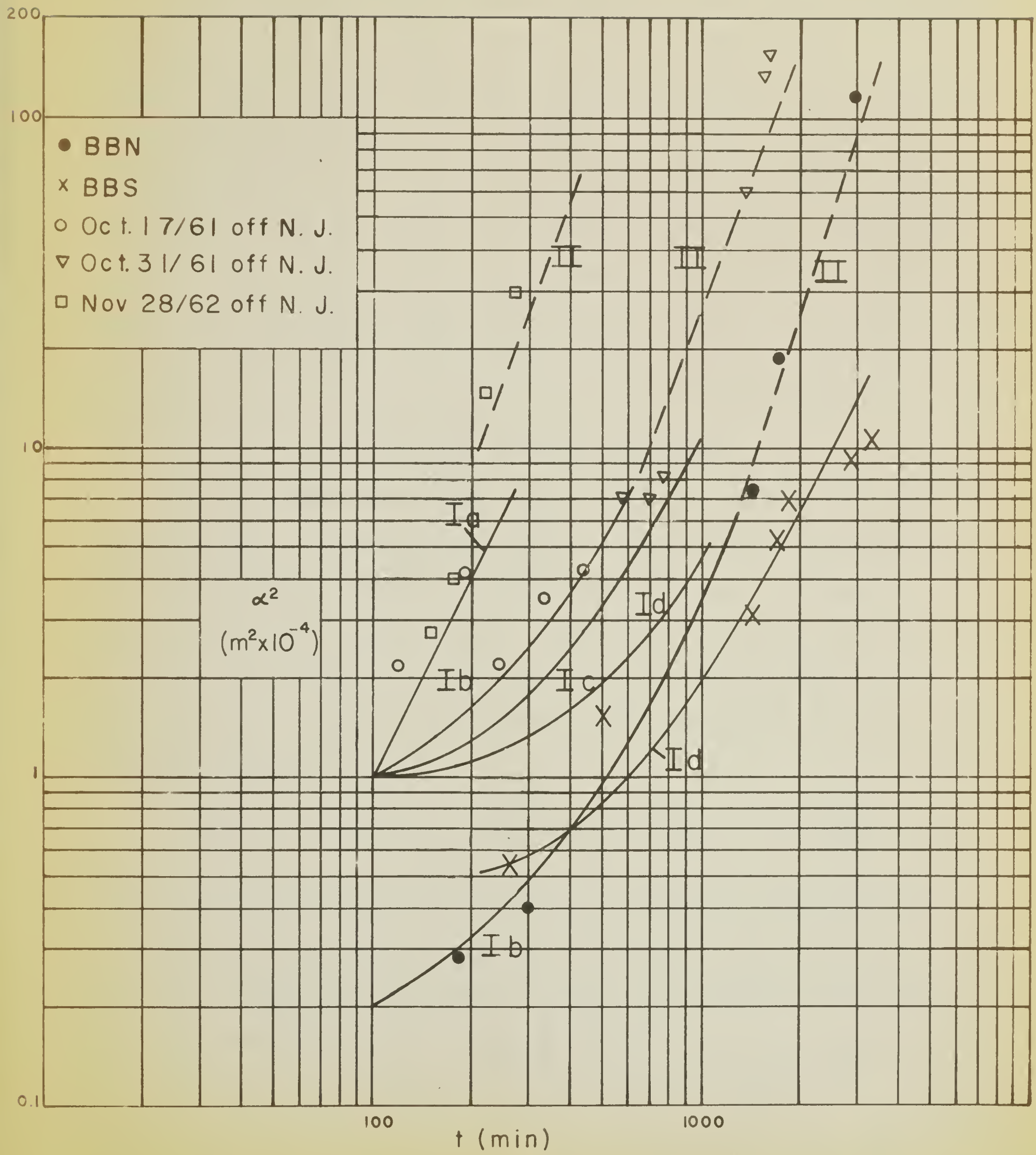

Ia, to = 0 Ic, to = 300 II ~ t^3

Ib, to = 200 Id, to = 500

FIGURE 1

III. ELONGATION AND CURVATURE OF DYE PATCHES

In many cases during the dye experiments, dye patches showed a tendency to elongate in a direction of surface currents, as described in ENY. Such elongation may be explained partly by anisotropy of turbulence, and partly by vertically differential advection of the mean flow. The first effect was verified experimentally in a shear flow of a flume, in which the large eddies are elongated in the direction of the mean flow (Townsend, 1956). Since the surface current, in most cases of the experiments, were generated by surface winds, there was a vertical shear near the surface. Thus, turbulent diffusion was usually stronger in the direction of the surface flow than in the lateral direction, although an accurate measurement of fluctuations of currents in the sea is yet to be done to verify this effect.

The second effect was usually more obvious in many experiments. Some aerial photographs clearly indicate that the leading portion of a patch with the highest concentration moves faster near the surface while the trailing portion lies below the surface, as often seen from a band of dye stirred up by crossing of a research vessel (Example, Figure 9 in ENY). Analytically, this type of dye distribution is expressed by a solution of the following diffusion equation:

$$\frac{\partial S}{\partial t} + U(z)\frac{\partial S}{\partial x} + V(z)\frac{\partial S}{\partial y} = A_x \frac{\partial^2 S}{\partial x^2} + A_y \frac{\partial^2 S}{\partial y^2} \qquad (1)$$

where S is the concentration, U(z) and V(z) are horizontal components of the mean flow, A_x and A_y are horizontal eddy diffusivity, and the vertical eddy diffusion is neglected. The solution of equation (1), corresponding to the initial source concentration F(x,y,z), is given by:

$$S(x,y,z,t) = (4\pi t)^{-1}(A_x A_y)^{-\frac{1}{2}} \int_0^{\infty}\int_0^{\infty} F(\alpha,\beta,z)\exp\left\{-\frac{(x-\bar{U}t-\alpha)^2}{4A_x t} - \frac{(y-Vt-\beta)^2}{4A_y t}\right\} d\alpha\, d\beta \qquad (2)$$

For the line source at the origin (x = y = 0), the solution is given by the integrand of (2) with F = 1 and $\alpha = \beta = 0$. Further, when V(z) = 0, the concentration in aerial photographs is represented by:

$$S'_a = \int_0^H S'(x, y, z, t)\, e^{-kz}\, dz$$

$$= (4\pi t)^{-1} (A_1 A_y)^{-\frac{1}{2}} \exp\left(\frac{-y^2}{4A_y t}\right) \int_0^H \exp\left\{-\frac{(x-Ut)^2}{4A_1 t} - kz\right\} dz \qquad (3)$$

in which k is a vertical extenction coefficient of dye in the water, and H is the depth. The concentration S_a is computed from equation (3) for the case of constant current ($U = U_0$) and for the case of vertically variable current $U = \frac{\pi}{2} U_0 \cos\frac{\pi}{2} z$ by taking k = 0. The result is schematically shown in Figure 2, in which the concentration is plotted with arbitrary units. The figure indicates that the dye patch becomes elongated owing to a long trailing part after a certain period.

IV. CURVATURE OF THE PATCHES

It was discovered in a number of experiments that the trailing portion of the dye patches showed a pronounced clockwise curvature from the source near the surface to the tail in increasing depth when the wind speed was fifteen knots or more (Gerard and Katz, 1963, hereafter cited as GK). Gerard and Katz considered that the curved tail of dye patches is caused by the effect of an Ekman spiral (actually, effect of differential advection due to the Ekman flow in the upper layer), owing to the fact that the trail is curved clockwise in most cases.

Another possible explanation for this phenomenon is the effect of refraction at the sea surface when an underwater object is observed from above.

FIGURE 2.

Concentration diagrams for an instantaneous point source either in a shear flow or in a uniform flow.

Non-dimensional parameters: $\xi = x\, U_0\, A^{-1}$,

$\eta = y\, U_0\, A^{-1}$, $\tau = t\, U_0^{\,2} A^{-1}$

The groups A, B, C, D and E represent the concentration at τ = 4.9, 9.7, 38.9, 58.3, and 87.5, respectively.

The subscripts 1 and 2 of each group indicate the concentration for the shear flow $U = \frac{\pi}{2} U_0 \sin \frac{\pi}{2} \frac{z}{h}$

and the uniform flow $U = U_0$, respectively.

Fig. 2a

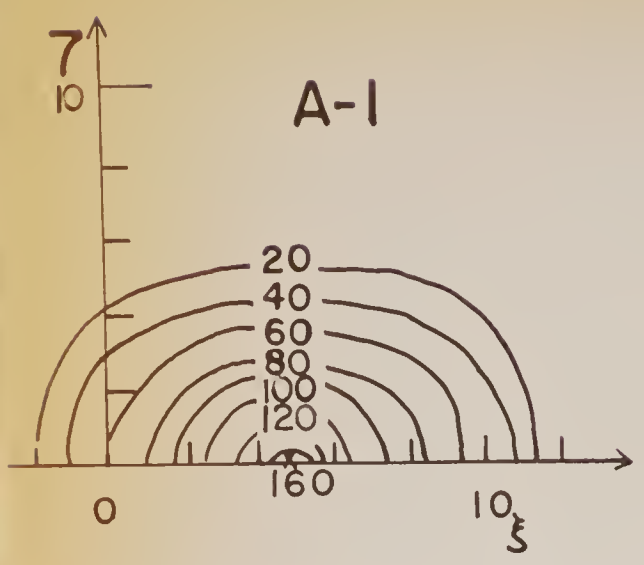
7
10
A-1
20
40
60
80
100
120
160
0
10
ξ

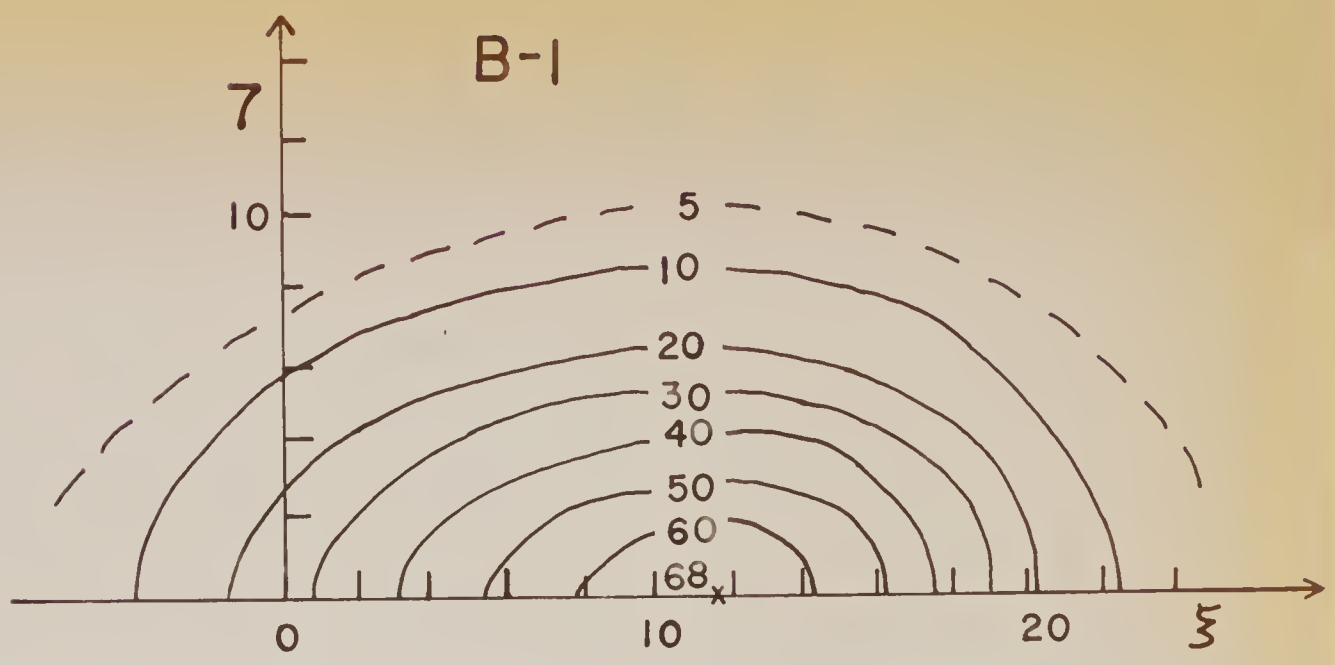
B-1
7
10
5
10
20
30
40
50
60
68
0
10
20
ξ

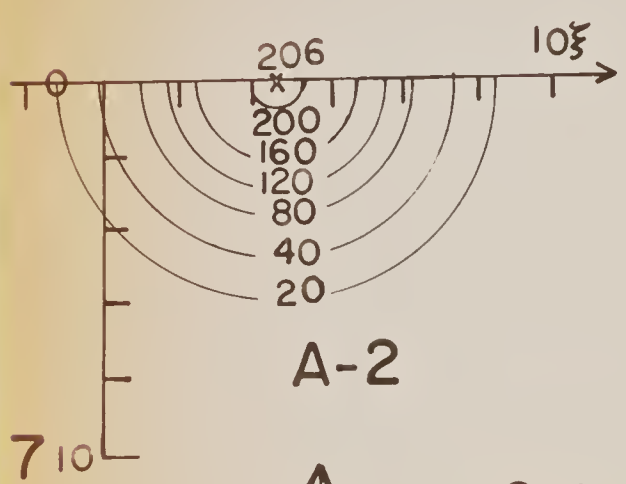
206
10ξ
0
200
160
120
80
40
20
A-2
7
10

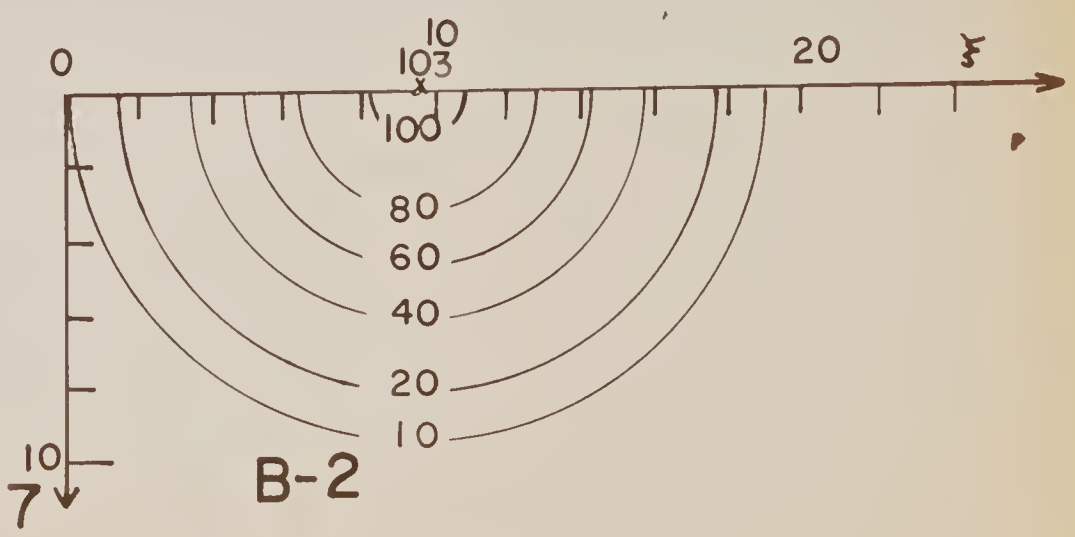
0
10
103
20
ξ
100
80
60
40
20
10
10
7
B-2

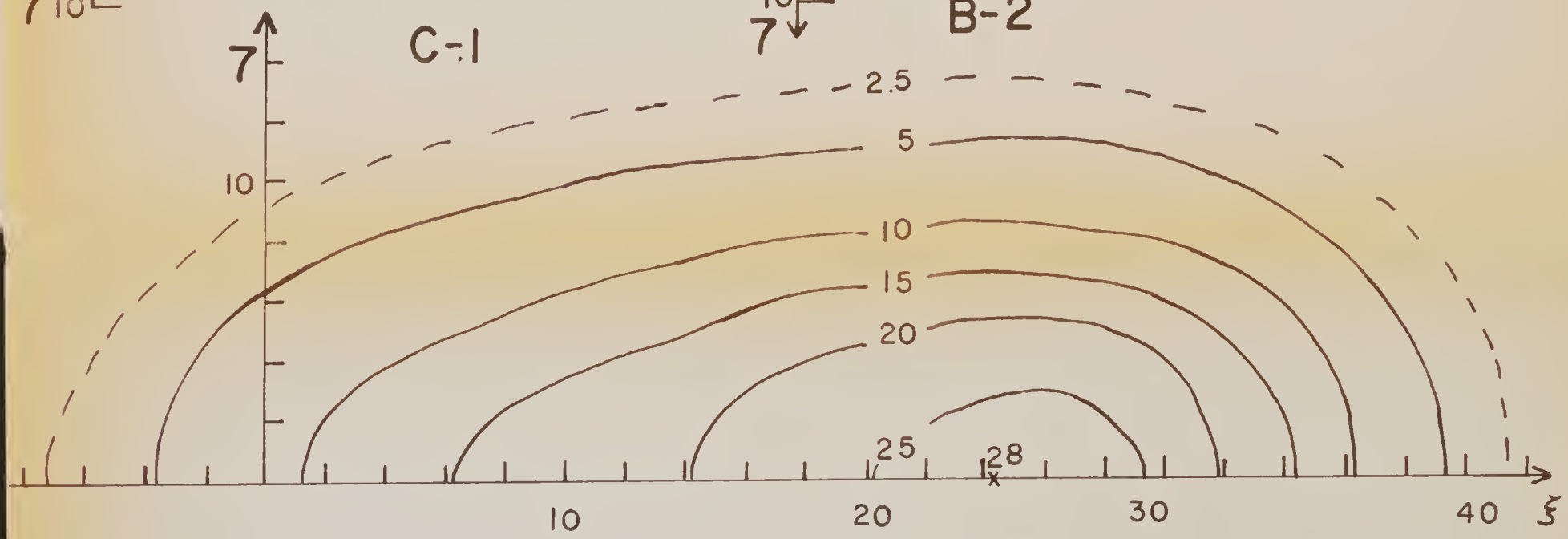
C-1
7
2.5
5
10
15
20
25
28
10
20
30
40
ξ

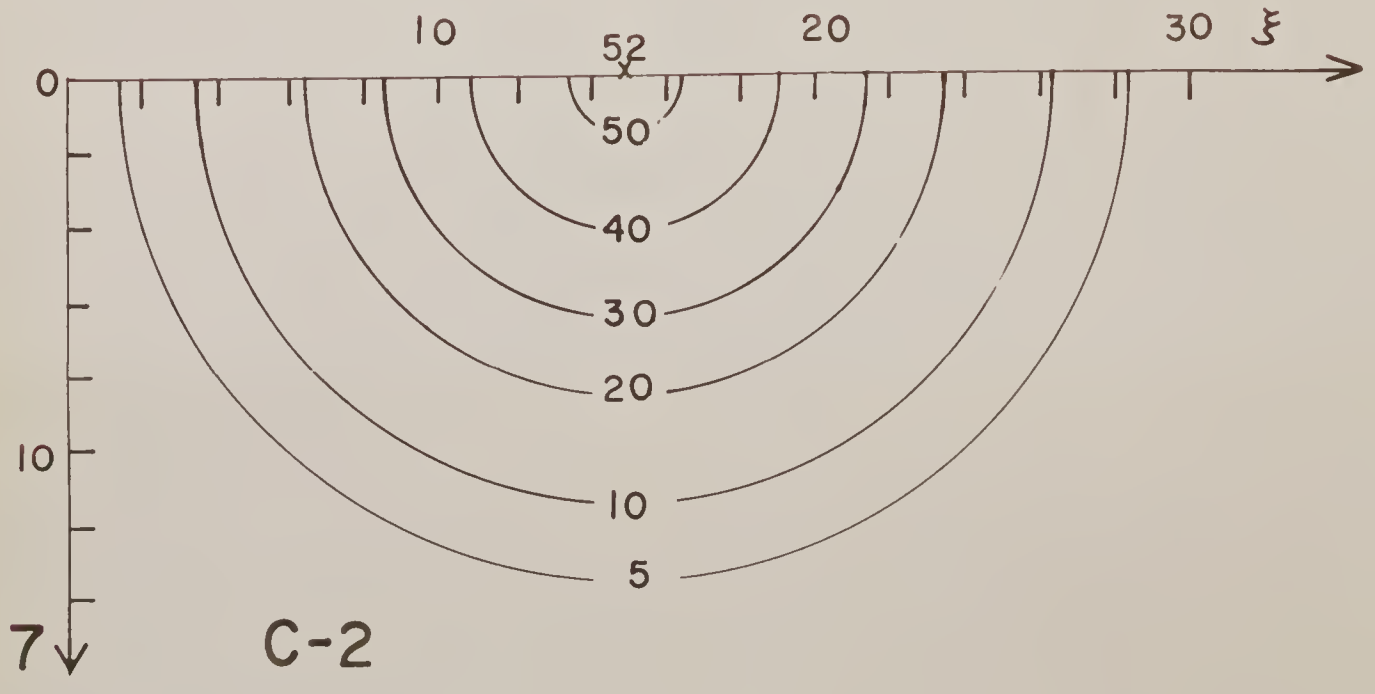
10
20
30
ξ
52
0
50
40
30
20
10
5
10
7
C-2

Fig. 2b

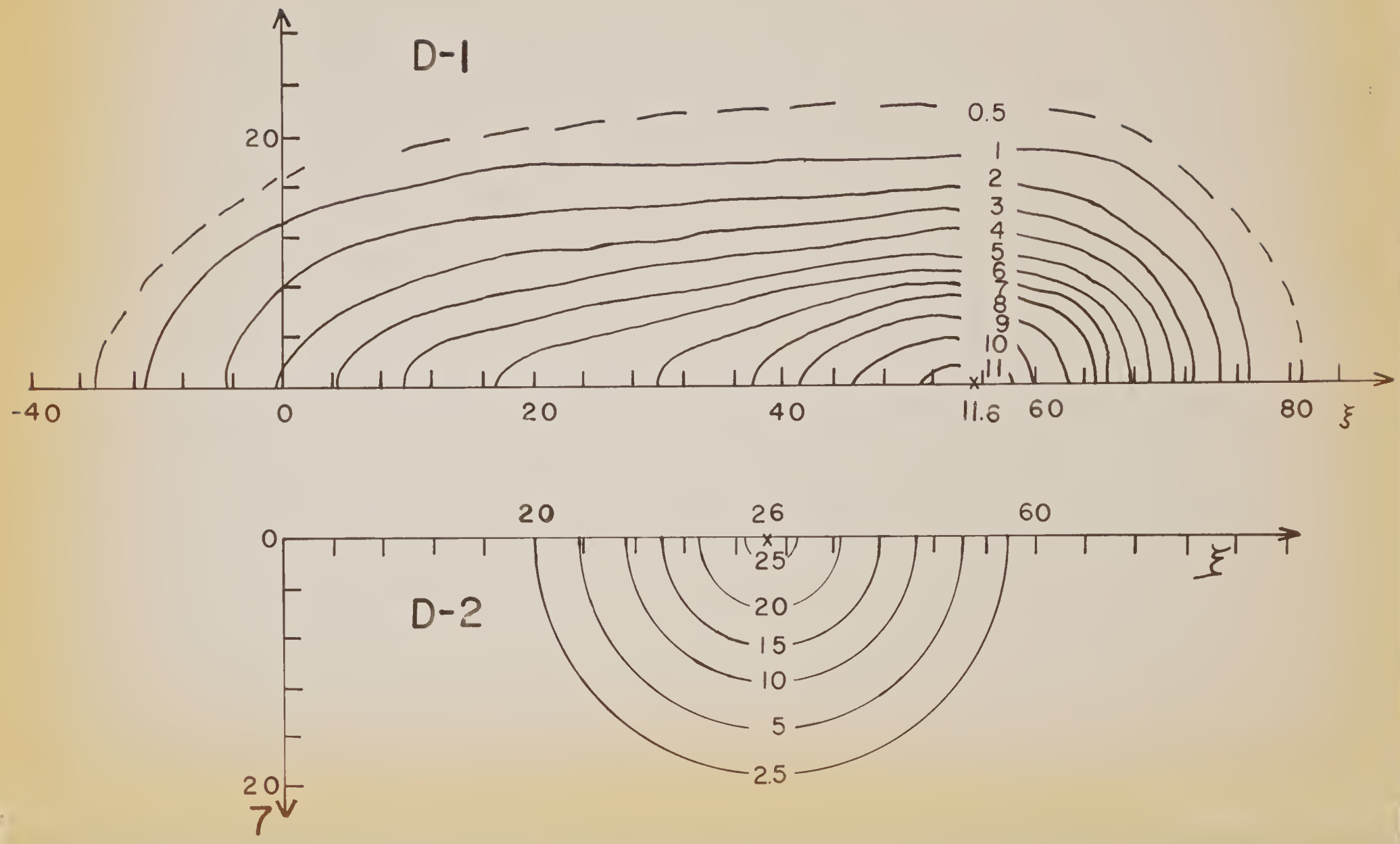
D-1
20
0.5
1
2
3
4
5
6
7
8
9
10
11
x
-40
0
20
40
11.6
60
80
ξ
20
26
60
0
25
20
15
10
5
2.5
D-2
20
7
40
7
E-1
0.5
1
2
3
4
5
6
7x
0
40
80
120
ξ

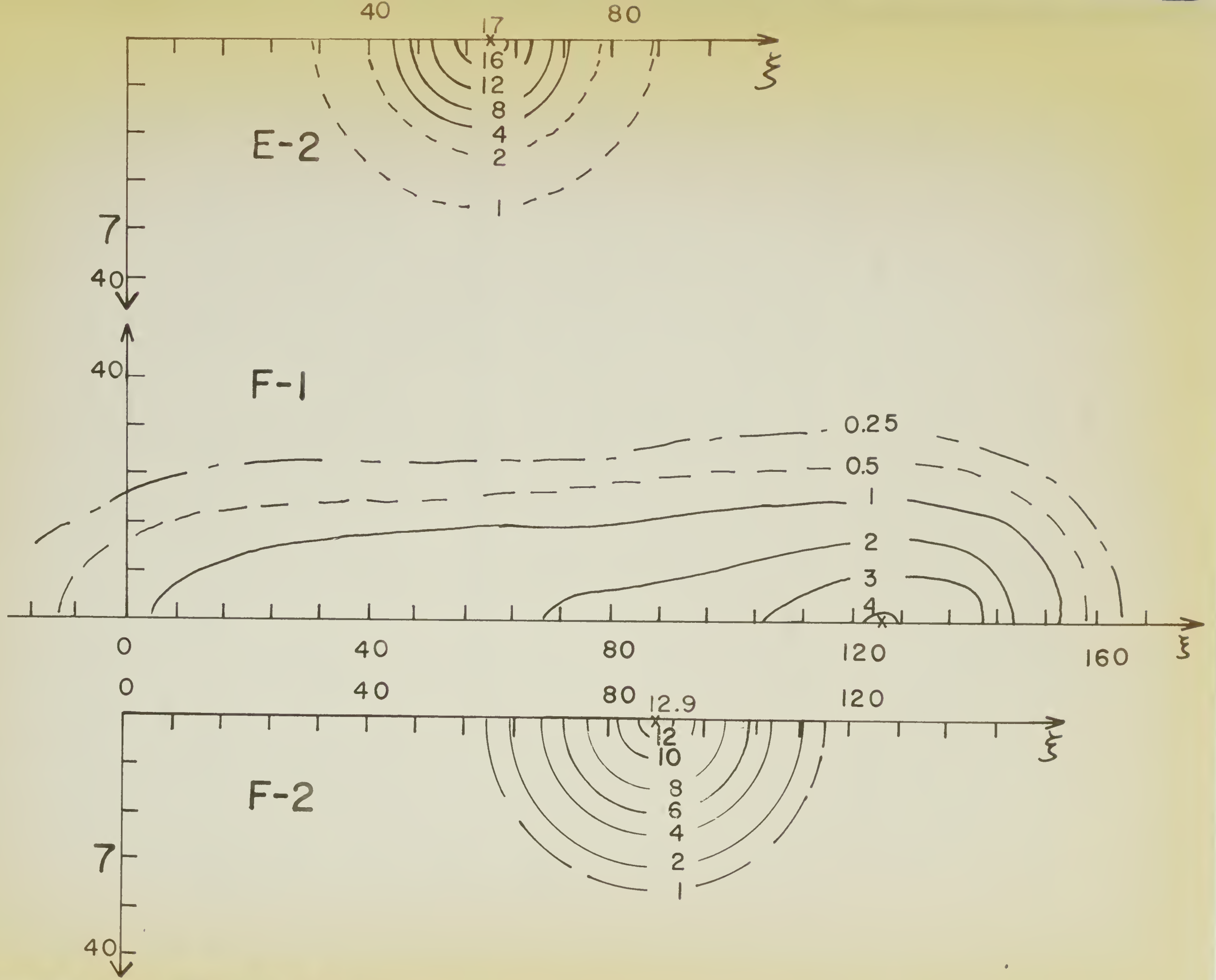
E-2
40
17
80
16
12
8
4
2
1
7
40
F-1
40
0.25
0.5
1
2
3
4
0
40
80
120
160
ξ
0
40
80
12.9
120
ξ
F-2
12
10
8
6
4
2
1
7
40

In order to determine this effect on curvature of the image at the sea surface, the geometrical arrangement of the object, image and camera (or eye) is shown in Figure 3. In this figure $P(x,y,z)$, $P'(X,Y,0)$, and $Q(x_o,y_o,z_o)$ are the underwater object, its image at the sea surface, and a camera, respectively. The points R and S are respective projection of P and Q on the sea surface. The angles of incidence and reflection are designated by θ' and θ, respectively.

Snell's law yields the following equations for X and Y:

$$X = x_o - z_o \frac{x_o - x}{\overline{RS}} \cdot \tan\theta \tag{1}$$

$$Y = y_o - z_o \frac{y_o - y}{\overline{RS}} \tan\theta \tag{2}$$

in which the distance $\overline{RS}$ is given by:

$$\overline{RS} = -z \tan\theta' + z_o \tan\theta \tag{3}$$

and there is the following relationship between θ and θ':

$$\frac{\sin\theta}{\sin\theta'} = n \tag{4}$$

in which n indicates the refractive coefficient of the sea water. When the position of the camera Q is fixed, the image P' can be determined from equations (1) and (2) by moving the point P on the object. In equations (1) and (2), θ is determined as a function of $P(x,y,z)$ from conditions (3) and (4).

In order to estimate the curvature of the image, let us consider a simple example in which a submerged straight bar extends with an angle from the sea surface (Figure 4). The origin of coordinates is taken at the intersection of the bar with the sea surface. It is assumed that the camera is located in the plane perpendicular to the bar, and its coordinates become $(0,L,\alpha L)$. When the angle of the bar with the sea surface is taken $-\gamma$, the coordinates

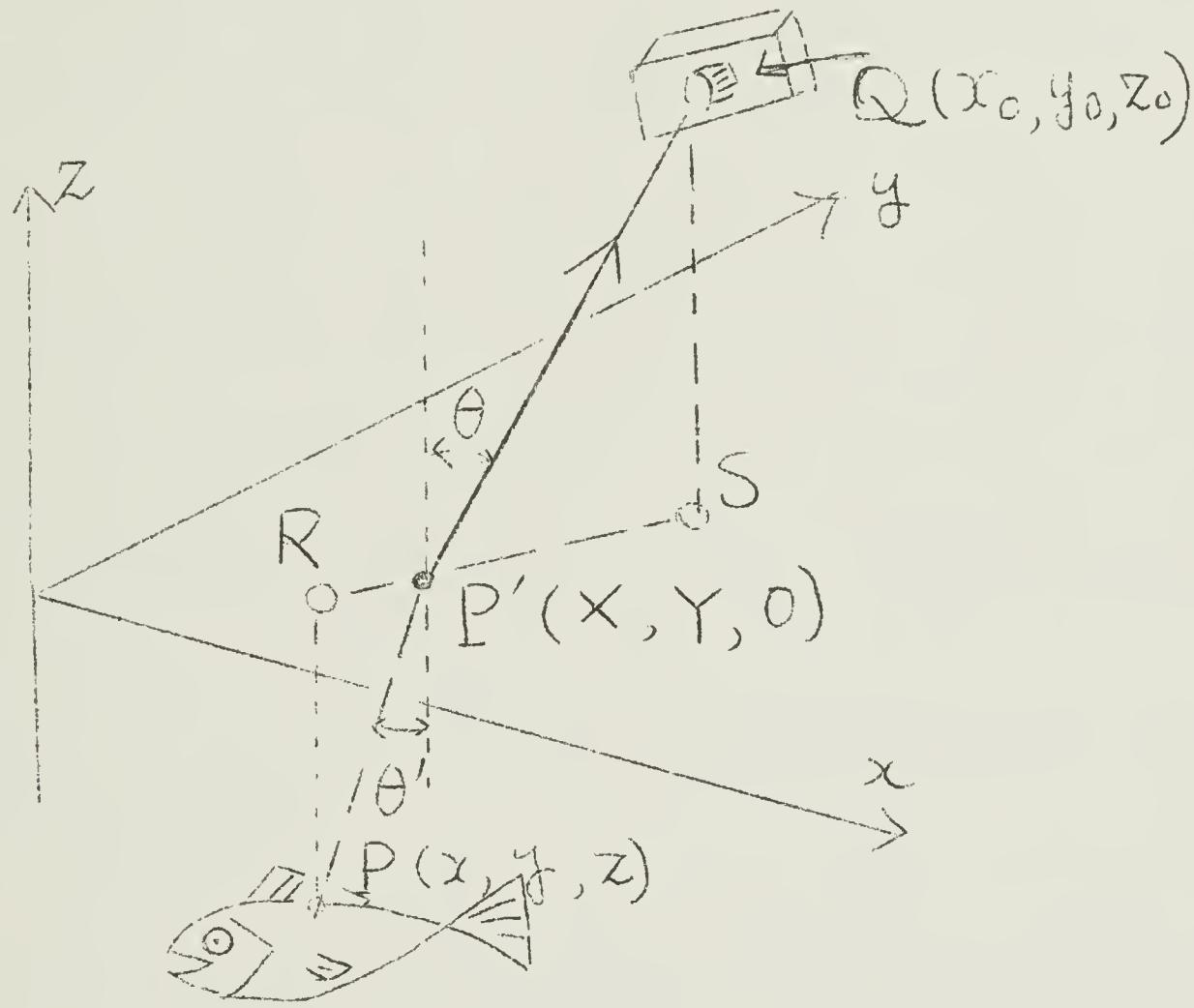

FIGURE 3

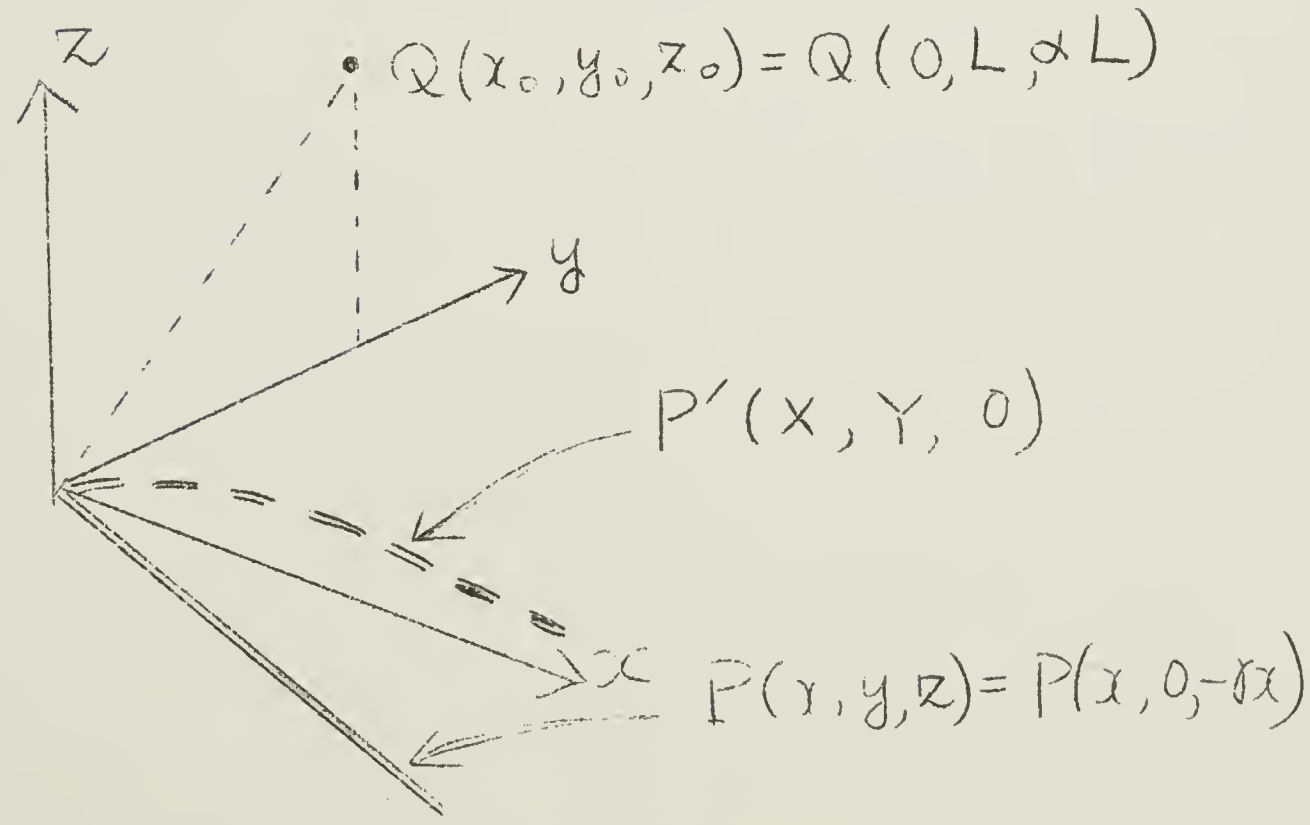

FIGURE 4

of the bar are given by $(x,0,-\gamma x)$. Eliminating x from (1) and (2) under the constraint conditions (3) and (4), we have:

$$X^2+(L-Y)^2=\frac{\alpha^2L^2}{n^2-1}\left\{\left(\frac{r}{\alpha}\right)^2\frac{X^2}{Y^2}-n^2\right\} \qquad (5)$$

as an equation for the curve of the image. At first sight this equation does not represent a straight line as is the underwater object. However, actual calculation of equation (5) indicates that the curve expressed by (5) is almost a straight line for nominal conditions of aerial photography of dye patches, as the following numerical example indicates. Figure 5 shows the computed image for $\alpha = 1$, $r = 0.1$, and $n = \sqrt{2}$, that is, when the angle of the camera with the object equals 45° and the submerged bar makes an angle of 5.7° with the sea surface.

When it is assumed that the curved trail of dye patches is caused by a vertically differential advection, we can compute distributions of vertical eddy viscosity of the mean current, if the curvature of the trail and the velocity and shear of the mean flow are known at each depth (Ichiye, 1963). The derivation of such relation is briefly discussed. In Figure 6 the distortion of a dye filament due to the differential advection is schematically shown. The origin of coordinates is taken at the sea surface. The hatched areas represent the dye filament at the initial time, and after time t. The coordinates ξ and η are projection of the dye filament on the sea surface. The components of the mean flow are expressed by $u(x,y,z,t)$ and $v(x,y,z,t)$. In order to simplify the problem, it is assumed that the diffusion of the dye filament is neglected. Then the movement of the filament is only due to the advection by the mean flow, and there are the following relations:

$$\frac{d\xi}{dt}=u(x,y,z,t)\ ;\quad \frac{d\eta}{dt}=v(x,y,z,t) \qquad (6)$$

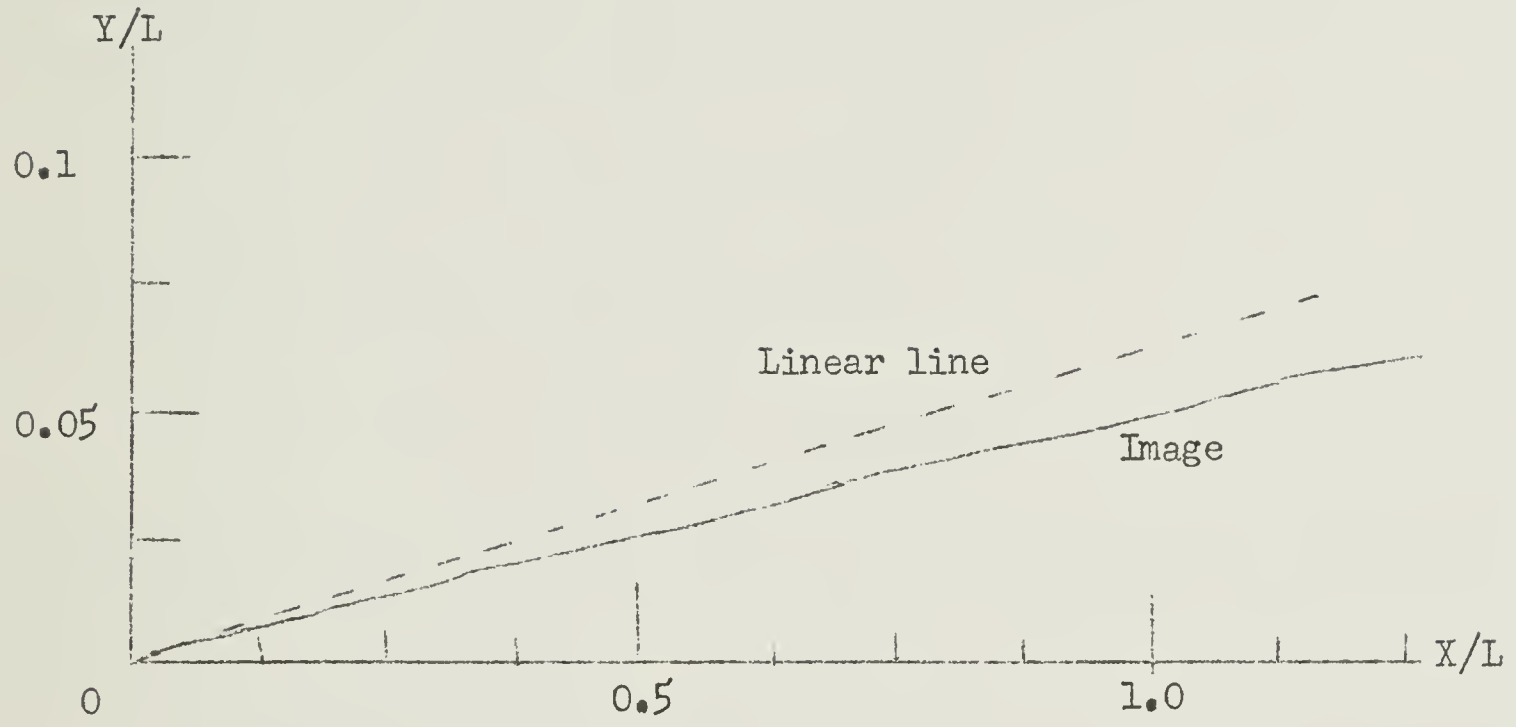

FIGURE 5

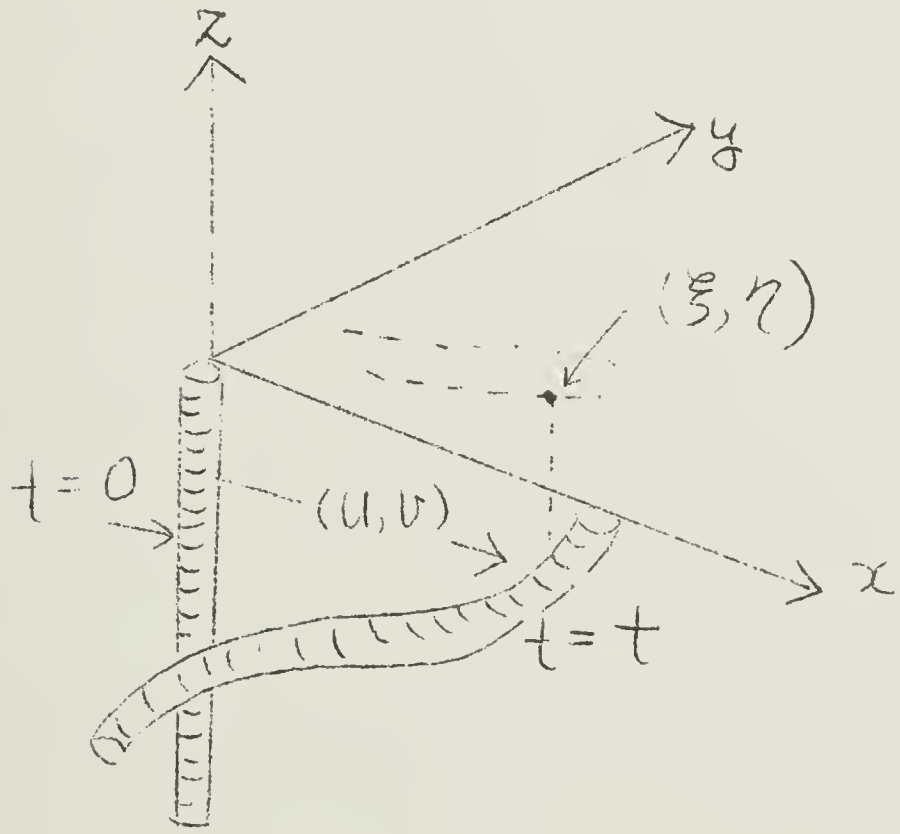

FIGURE 6

The radius of the curvature of the projected curve is designated by R(s), in which ds is a line element defined by:

$$ds^2 = d\xi^2 + d\eta^2 \tag{7}$$

A theorem of differential geometry yields:

$$R^{-1}(s) = |d^2\vec{r}/ds^2| \tag{8}$$

in which $\vec{r}$ is the radial vector (ξ, η). Since it is more convenient to express R(s) as a function of the argument z, we have the following equation:

$$R(z)^{-1} = |\eta_z \xi_{zz} - \xi_z \eta_{zz}|(\xi_z^2 + \eta_z^2)^{-\frac{3}{2}} \tag{9}$$

In the stationary Ekman flow, the components of the mean current satisfy the following equations:

$$-fv = \frac{d}{dz}\left\{K(z)\frac{du}{dz}\right\}, \quad fu = \frac{d}{dz}\left\{K(z)\frac{dv}{dz}\right\} \tag{10}$$

in which K(z) is the vertical eddy viscosity variable with depth and f is Coriolis' parameter. The values of ξ and η, obtained by integrating (6), simply equal the velocity multiplied with time, because u and v are dependent only on z. Substitution of these values of ξ and η into (9) yields:

$$K(z) = f R(z) \frac{d}{dz}(u^2+v^2) \cdot t^{-1} (u_z^2 + v_z^2)^{-\frac{3}{2}} \tag{11}$$

This equation indicates that we can determine the vertical eddy viscosity at any depth if we know the curvature of the projection of dye filament R(z), the mean flow u and v, and the shear u_z and v_z.

Application of equation (11) to the dye patches in the previous experiments is limited because of uncertainty of the depth of the trailing part.

However, if we assume that the eddy viscosity is almost uniform in the upper ten meters, the aerial photographs taken at 1326 on October 19, 1961 (ENY, GK) can be used for estimation of the eddy viscosity. In this example, the velocities u and v have an order of magnitude of 10 cm/sec, the shear u_z and v_z of $10^{-2}sec^{-1}$, t is 10^4 sec, and the average radius of curvature estimated from the photograph is about 10^5 cm. When these values are used, equation (11) yields the vertically averaged value of K(z) equalling about 10^2 cm^2/sec, which is quite reasonable compared with other estimation of the vertical eddy viscosity (Ichiye, 1962b).

V. STRIATION OF DYE PATCHES

Another remarkable feature observed in many experiments is striation (sometimes split into several blocks) of dye patches (ENY; Ichiye, 1962a). Two possible causes of this phenomenon were discussed in the previous paper (Ichiye, 1963). One is a hypothesis on mechanism of natural streaks proposed by Welander (1963). The other is the roll-type instability in rotating tank experiments by Faller (1963). The striation of dye patches has more regular and wider spacings (an order of 100 m) and deeper penetration (a few tens of meters) than natural streaks or Langmuir streaks. Therefore, Welander's model is hardly applicable to the present phenomenon. In fact, Reynolds' number of a rotating boundary layer $v(\nu\Omega)^{-\frac{1}{2}}$ equals about 300 for a number of experiments, in which $v \approx 10$ cm/sec, $\nu = 0.1$ cm^2/sec, and $\Omega = 10^{-4}sec^{-1}$. The fact that this value is far above the critical Reynolds' number 150, above which the roll-type instability starts in Faller's experiments, seems to be favorable to the cause due to instability.

The third possible cause of striation is the effect of waves producing rolling-up of a filament of dye, as discovered by Hama (1962) by numerical

integration of streaklines. He showed that the streaklines (filaments of dye injected constantly from a fixed source) become rolled up into a number of apparent discrete vortices near the critical layer where the mean shear flow, given by:

$$U_0 = 1 + \tanh y \tag{1}$$

has zero curvature ($y = 0$), due to unamplifying travelling sinusoidal waves superimposed on this shear flow. It is noted that many cases of striation were observed when there were swells and winds were rather high. This suggests that the swells and the wind drift may provide the same effect as the shear flow and the perturbation superposed on it, as postulated in Hama's model. Also, since the main part of the dye patches was large compared with individual striated patterns, the dye is considered to be fed continuously to the streaklines. It would be an interesting problem to test the applicability of Hama's theory to striation by future field experiments.

ACKNOWLEDGMENTS

The authors wish to thank Robert Gerard, Michael Costin and Bernard Katz for freely supplying them with information and data from their field experiments. The cooperation of Dr. James Dorman in programming the computation of equation III(3) for IBM 1620 is also greatly appreciated

The work reported in this paper was supported in part by the Atomic Energy Commission of the U. S. Government under Contract AT(30-1)2663.

REFERENCES

Batchelor, G. K., 1950. The application of the similarity theory of turbulence to atmospheric diffusion: Quart. J. R. Met. Soc. 76, 133-146.

Batchelor, G. K., 1953. The Theory of Homogeneous Turbulence: Cambridge Univ. Press.

Batchelor, G. K. and A. A. Townsend, 1956. Turbulent diffusion: Surveys in Mechanics, ed. by G. K. Batchelor and R. M. Davies, Cambridge Univ. Press.

Costin, M., 1963. Dye diffusion experiments on the Bahama Banks: Tech. Rep. No. CU-6-63, Lamont Geological Obs. of Columbia Univ. (unpublished manuscript).

Costin, M., P. Davis, R. Gerard and B. Katz, 1963. Dye diffusion experiments in the New York Bight: Tech. Rep. No. CU-2-63, Lamont Geol. Obs. of Columbia Univ. (unpublished manuscript).

Faller, A. J., 1963. An experimental study of the instability of the laminar Ekman boundary layer: J. Fluid Mech. 15, 560-576.

Frenkiel, F. N., 1958. Comparison between molecular and turbulent diffusion processes: Proceedings of the International Symposium on Transport Processes in Statistical Mechanics, Ed. by I. Prigogine, 204-214, Interscience Publishers, Inc.

Frenkiel, F. N., 1962. Introduction to international symposium on fundamental problems in turbulence and their relation to geophysics: J. Geophys. Res. 67 (8), 3007-3010.

Gerard, R. and B. Katz, 1963. A note on some observations of dye in coastal waters: Tech. Rep. No. CU-3-63, Lamont Geol. Obs. of Columbia Univ. (unpublished manuscript).

Gifford, F., 1957. Relative atmospheric diffusion of smoke puffs: J. Met. 14, 410-416.

Hama, F. R., 1962. Streaklines in a perturbed shear flow: Physics of Fluids 5(6), 644-650.

Ichiye, T., 1962a. Studies of turbulent diffusion of dye patches in the ocean: J. Geophys. Res. 67, 3212-3216.

Ichiye, T., 1962b. Oceanic turbulence (review): Tech. Paper No. 2 for ONR, pp. 200 (unpublished manuscript).

Ichiye, T., 1963. Some comments and prospectives on dye diffusion experiments: Technical Note at AEC and ONR, Lamont Geol. Obs. of Columbia Univ. (unpublished manuscript).

REFERENCES - (continued)

Townsend, A. A., 1956. The Structure of Turbulent Shear Flow, Cambridge Univ. Press.

Welander, P., 1963. On the generation of wind streaks on the sea surface by action of surface film: Tellus 15, 33-43.